Operational VGOS Scheduling

Anthony Searle[1], Bill Petrachenko[1,2]

Abstract The VLBI Global Observing System (VGOS) has been designed to take advantage of advances in data recording speeds and storage capacity, allowing for smaller and faster antennas, wider bandwidths, and shorter observation durations. Here, schedules for a "realistic" VGOS network, frequency sequences, and expanded source lists are presented using a new source-based scheduling algorithm. The VGOS aim for continuous observations presents new operational challenges. As the source-based strategy is independent of the observing network, there are operational advantages which allow for more flexible scheduling of continuous VLBI observations. Using VieVS, simulations of several schedules are presented and compared with previous VGOS studies.

Keywords VGOS, operations, scheduling

1 Introduction

Since the publishing of the VLBI2010 specification [1], many countries have invested in new VLBI antennas that adopt the new standard. In the coming years, a global network of these smaller, fast antennas will become available for VGOS operations. This new mode of operation will require re-evaluating how stations are scheduled and how to make optimal use of their new capabilities. Further, the new frequency regime will affect source selection and observation lengths. There remains a question of how many sources exist that can be observed over the new wide bandwidths. Here we present a simulation using four different prospective frequency sequences and a simulation using source lists of various sizes. Both simulations use a scheduling algorithm that is designed to maximize observations while minimizing station bias.

1. Natural Resources Canada, Canadian Geodetic Survey
2. Dominion Radio Astrophysical Observatory

2 Source-Based Scheduling

Because VGOS will operate using expanded frequency bandwidths and smaller, fast antennas, scan durations will be shorter and observations more frequent. The "opposite sky" source-based scheduling algorithm used in this study aims to maximize observations at each site, independent of the ground network.

The scheduling algorithm randomly selects a source that has not been observed recently and then selects a second source roughly opposite on the sky. A majority of stations should be able to observe one of the two sources and each station joins the observation if it is able to slew there in time. A new set of sources is selected every 30 seconds. Sources are chosen so that sources have an equal number of observations.

Scan duration was calculated using the correlated flux for the source, the antenna/receiver sensitivity, and the frequency sequence. Because it was shown that geodetic/astrometric performance does not degrade significantly until delay measurement error exceeds 16–32 ps [2], there was no attempt to improve delay precision beyond 8 ps. As a result the calculation of integration time, Δt, was divided into three regimes, i.e.,

If $SCsrc < S8ps$ then $\Delta t = 10s$

$$\text{If } SCsrc > S8ps \text{ then } \Delta t = 10s(S8ps/SCsrc)^2$$
$$\text{If } \Delta t < 1s \text{ then } \Delta t = 1s$$

where $SCsrc$ is the correlated flux of the source and $S8ps$ is the correlated flux at which a particular frequency sequence achieves 8 ps delay precision. In addition to the scan duration, a three second buffer was added to each scan to allow each antenna time to “settle” and acquire the source.

There are operational advantages in using a simple scheduling algorithm:

- An algorithm that is unaffected by the ground network is easier to operate; stations can drop out with minimum influence on the schedule and rejoin as soon as they are available.
- The fastest sites are used more effectively. More complicated schemes have to decide whether to wait for slower dishes, which tends to prioritize the slower dishes.
- More sparsely populated hemispheres are observed at the same rate as densely occupied regions. Algorithms that maximize observations prefer dense parts of the network.

Prerequisites for a source based solution to work effectively include a globally distributed ground network and a well-distributed source list.

3 VGOS Simulation Network

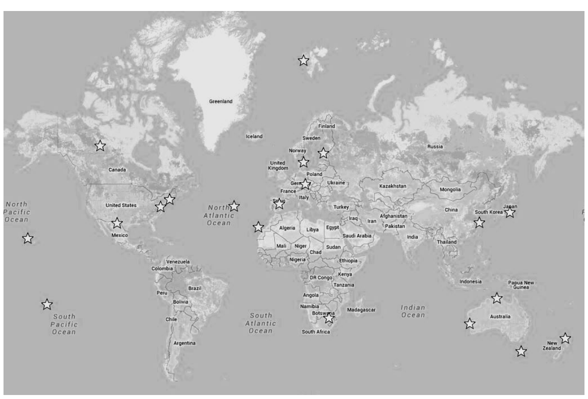

Fig. 1 VGOS simulation network.

The VGOS simulation network which includes 19 sites that are either built, under construction, or planned, plus a Yellowknife station, can be seen in Figure 1. Up-to-date antenna specifications are used for known antennas; VGOS specifications are used for anticipated sites (see Table 1). The antenna distribution is quite good, but there are notable gaps in South America, Russia, and the Middle East. Europe and the eastern United States have some short baselines, but these may be valuable if regular imaging of radio sources becomes part of VGOS operations.

Table 1 Station characteristics of VGOS network.

Station Name	Az. Rate (deg/min)	El. Rate (deg/min)	$C_n x10^{-7}$ $m^{-1/3}$
KOKEE12M	720	360	1.78
WETTZ13S	720	360	1.8
WESTFORD	720	360	3.67
NYALES12	720	360	0.95
ISHIOKA	720	360	2.3
HART12M	720	360	1.47
ONSALA12	720	360	2.09
GGAO12M	300	66	2.3
HOBART12	300	75	1.6
KATH12M	300	75	1.68
METSA12M	720	360	2.09
MCD_12M	720	360	1.45
RAEGCANA	720	360	1.5
RAEGFLOR	720	360	1.5
RAEGYEB	720	360	1.5
SESHA12M	720	360	1.79
TAHIT12M	720	360	2.19
WARK12M	300	60	1.6
YARRA12M	300	75	1.76
YELLOW12	720	360	1.24

4 Frequency Sequence Simulation

The VGOS system will use four bands of frequencies in the 3–14 GHz range. The exact placement of the frequencies has not yet been determined. It is known that the frequency sequence will affect the scheduling by varying the scan durations for a target delay precision and limiting the ability to connect the phase across the observing band for weaker sources.

To investigate the effect of the frequency sequence on scheduling, four prospective VGOS frequency sequences were used to create day-long schedules using the sky-based algorithm and the 128-source list from the source number simulation (see Section 5). In order to determine scan lengths for each sequence, minimum source fluxes for which the delay observable

Table 2 Characteristics of frequency sequences.

Sequence number	Min Flux (mJy)	Avg $\Delta\tau$ (ps)	SNR @min	Flux for 8ps (mJy)	BW (MHz)	Data Rate(Gbps)	Number of Scans	# Obs.	F1 (MHz)	F2 (MHz)	F3 (MHz)	F4 (MHz)
1	80	9.36	10	208	1024	31.7	5710	165644	3008	4896	8288	9696
2	110	11.129	10	255	1024	16.4	5701	159610	3008	5062	6688	9696
3	130	11.194	12	148	1024	16.4	5706	161398	3008	5792	8032	12704
4	190	11.426	17	290	512	15.4	5683	156841	3008	4960	7872	9280

uncertainty would equal 8 ps in 10 seconds (see Table 2), were determined (see Section 2). Observations were simulated with a turbulent troposphere with Treuhaft-Lanyi parameters and site-dependent structure constants taken from Sun [3] (see Table 1); clocks were modeled with Allan Standard Deviations of $1\text{x}10^{14}$ at 50 minutes, and the delay measurement precision was determined by the flux method described in Section 2.

Least-squares parameter estimations of EOPs, site positions, tropospheric parameters, and site clocks were completed using VieVS [4]. Zenith troposphere delay offsets were determined at 15-minute intervals with a piece-wise linear constraint of 15 mm between adjacent offsets; gradients were estimated at 30-minute intervals with 1 mm absolute constraints; clocks were determined as second order polynomials with linear offsets determined every hour relatively constrained to 13 mm, and station positions were determined once per 24 hours constrained with no-net-rotation and no-net-translation conditions. EOPs were determined once per day.

5 Source Number Simulation

To study the impact of the number of sources available in the source list, five prospective source lists of varying length were used to produce day-long schedules using the "opposite sky" source-based algorithm and frequency sequence number 2 from Table 2. Source catalogs of 32, 64, 128, 256, and 512 sources were subsets of the Bordeaux VLBI Image Database [5] with sources with declinations below −45 degrees added from the Goddard Space Flight Center SKED source list [6]. The catalogs were determined by adjusting a cut-off minimum flux and maximum median delay error until the desired number of sources was included.

Observations were simulated using the same troposphere, clock, and noise models as in Section 4. EOPs, site positions, tropospheric parameters, and site clocks were determined using least-squares parameter reduction with the same strategy as in Section 4.

Table 3 Characteristics for source schedules.

	32	64	128	256	512
#Scans	5723	5696	5701	5679	5695
#Obs.	180119	163948	159610	151764	140882
Avg $\Delta\tau$ (ps)	8.248	10.06	11.129	12.586	13.737

6 Results

Station positions were determined for each schedule. For the frequency sequence simulation, the mean 3D rms station position scatter was 0.88, 0.93, 0.88, and 0.89 mm for sequences 1, 2, 3, and 4, respectively. In the source list size simulation the mean 3D rms station postion scatter was 1.08, 0.91, 0.93, 0.90, and 0.96 mm for the 32, 64, 128, 256, and 512 source lists, respectively. In both simulations, larger values of station position uncertainty corresponded to stations with slower slewing speeds and fewer observations.

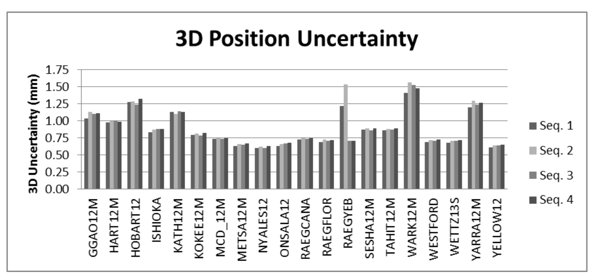

Fig. 2 3D rms of stations in frequency sequence study.

The EOP estimate formal uncertainty is shown in Table 4 for the different frequency sequence schedules and in Table 5 for different source lists. EOP determi-

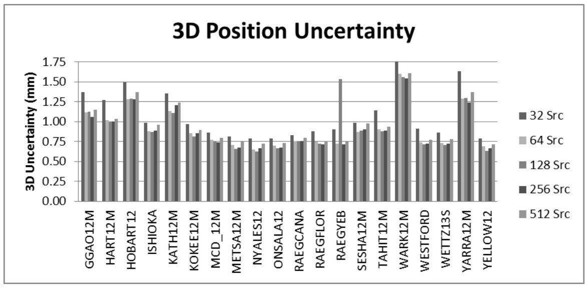

Fig. 3 3D rms of stations in source number study.

Table 4 EOP uncertainty for sequence simulations.

	Seq. 1	Seq. 2	Seq. 3	Seq. 4
Xp(μas)	3.68	3.84	3.71	3.77
Yp (μas)	3.74	3.87	3.84	3.83
dUT (μs)	0.178	0.183	0.184	0.184
dX (μas)	2.57	2.64	2.63	2.67
dY (μas)	2.56	2.63	2.61	2.65

Table 5 EOP uncertainty for source simulations.

	Source Number				
	32	64	128	256	512
Xp(μas)	4.25	3.68	3.84	3.89	4.10
Yp (μas)	4.39	3.79	3.87	3.97	4.19
dUT (μs)	0.210	0.184	0.183	0.187	0.195
dX (μas)	2.94	2.76	2.64	2.78	2.97
dY (μas)	2.93	2.60	2.63	2.77	2.95

nation appears to be insensitive to sequence, though there was a small degradation in EOP results for the 32 and 512 source lists.

7 Conclusions

- Neither the frequency sequence nor the source list had significant impact on the geodetic parameters of interest. Geometry and observation density are more important factors.
- Sites with greater than ∼13000 observations per day have position uncertainties of less than 1mm, which is a goal of VGOS.
- While the 32 source list schedule has the most observations, the limited geometry degraded the results. As the number of sources increased beyond 256, solutions become marginally worse due to the addition of a number of weaker sources resulting in fewer observations.
- After approximately 100 sources, the geometry is sufficient for station positions and EOPs, though there may be other reasons to expand the source list.
- Position determination was worse for the southern stations because many of the antennas in the south are slower and miss scans due to slewing.
- Operationally, having observations at regular intervals reduces complications in scheduling while increasing the number of observations and eliminating station and hemisphere bias.
- As the VGOS network matures, proper estimates of observation interval and scan duration could further improve the technique.

Acknowledgements

This research has made use of material from the Bordeaux VLBI Image Database (BVID).
http://www.obs.u-bordeaux1.fr/BVID

References

1. B. Petrachenko, A. Niell, D. Behrend, B. Corey, J. Böhm, P. Charlot, A. Collioud, J. Gipson, R. Haas, T. Hobiger, Y. Koyama, D. MacMillan, T. Nilsson, A. Pany, G. Tuccari, A. Whitney, J. Wresnik, “Design Aspects of the VLBI2010 System. Progress Report of the VLBI2010 Committee”. NASA Technical Memorandum, NASA/TM-2009-214180, 58 pp., June 2009.
2. D. MacMillan, J. Böhm, J. Gipson, R. Haas, A. Niell, T. Nilsson, A. Pany, B. Petrachenko, and J. Wresnik, “Simulation Analysis of the Geodetic Performance of the Future IVS VLBI2010 System”, 2008 Fall AGU poster, 2008. http://lupus.gsfc.nasa.gov/files_presentations/2008_fall_agu_v2c.ppt
3. J. Sun, J. Böhm, T. Nilsson, H. Krásná, S. Böhm, and H. Schuh, “New VLBI2010 scheduling strategies and implications on the terrestrial reference frames”, J. Geodesy 88:449-461. doi 10.1007/s00190-014-0697-9, 2014.
4. J. Böhm, S. Böhm, T. Nilsson, A. Pany, L. Plank, H. Spicakova, K. Teke, and H. Schuh, “The New Vienna VLBI Software VieVS”, In S. Kenyon, C. M. Pacino, and U. Marti, editors, “Geodesy for Planet Earth: Proceedings of the 2009 IAG Symposium, Buenos Aires, Argentina, 31 August — 4 September 2009”, Springer Berlin Heidelberg, Berlin, Heidelberg, pages 1007–1011, doi 10.1007/978-3-642-20338-1_126, 2012.
5. A. Collioud, P. Charlot, “The Bordeaux VLBI Image Data base”, 19th EVGA working meeting proceedings, G. Bourda, P. Charlot, and A. Collioud editors, 2009.
6. ftp://gemini.gsfc.nasa.gov/pub/sked/catalogs/source.cat, accessed January 18, 2016.